Leading-edge vortex stability in insect wings

F. O. Minotti and E. Speranza
Instituto de Física del Plasma, INFIP-CONICET, Departamento de Física, Universidad de Buenos Aires, 1428 Buenos Aires, Argentina
(Received 26 August 2004; revised manuscript received 16 November 2004; published 25 May 2005)

An analytical study is presented to determine if the persistency of the leading-edge vortex in an insect wing can be explained as the balance between vorticity generation at the leading edge and advection plus effects of vorticity stretching and tilting by the flow along the wing span. It is found that a spanwise flow of the required magnitude is produced by the simple rotation of the wing about its root at a constant angle of attack (no supination or pronation), and that the regions where this equilibrium exists in stable form are well localized, independent of the rotation velocity, almost independent of the position along the wing, and weakly dependent on the angle of attack, for angles below $\simeq 70°$. In contrast, extended regions of vorticity are expected for angles of attack above $\simeq 75°$.

DOI: 10.1103/PhysRevE.71.051908 PACS number(s): 87.19.St, 87.10.+e

I. INTRODUCTION

One particularly intriguing aspect of insect flight is the persistence of leading-edge vorticity against its tendency to be swept by the flow around the insect wing. The resulting leading-edge vortex (LEV) regularizes the flow over the wing at high angles of attack, and also increases the achievable lift [1]. Different mechanisms have been proposed to explain the persistence of the LEV. On the one side, the effective angle of attack is greatly reduced, compared to the geometrical one, by the downflow generated by tip vortices and wake, thus reducing the tendency towards instability [2]. On the other side, the flow along the wing span takes energy from the vortex core to compensate for that generated at the leading edge, thus producing an almost stationary LEV [3,4]. Both mechanisms, most certainly, play a part, and in this highly nonlinear, genuine three-dimensional problem their study is very difficult, including the interpretation of detailed numerical simulations in which the LEV stability is observed [5,6].

In the present work we explore the possibility of stabilization by action of the spanwise flow alone. Several approximations are required to tackle this problem analytically. First, we use the experimental [2] and theoretical [7] information that the flow over the wing has strong two-dimensional features, with highly concentrated regions of vorticity, which are then modeled as point singularities of a potential flow. Second, taking advantage of the relatively high Reynolds numbers involved in insect flight [8], inviscid potential theory is used to determine the flow around the wing, and Kutta-Joukowski conditions are used to evaluate circulations and emission of vorticity from the leading edge. These are the main approximations, followed by other approximations of more technical nature that will be indicated when needed. The main conclusion is that, for a given wing, a localized region of stable equilibrium between generation and effect of the spanwise flow exists that is independent of the rotation velocity, and practically independent of spanwise position, it only depends, and rather weakly, on the angle of attack for not too large angles (below $\simeq 75°$).

II. THREE-DIMENSIONAL FLOW IN ROTATING WINGS

Let us consider a flat wing of chord length $D(z)$ that rotates with constant angular velocity $\vec{\mathbf{\Omega}}_T$ about a fixed axis (Fig. 1). The rotation axis and the normal to the plate are at a constant angle α, so that the wing attacks the fluid with this angle as it rotates, with the fluid at rest far away. We take comoving Cartesian coordinates (x,y,z) with x along the wing chord and with y normal to it, such that $x=-D(z)/2$ corresponds to the leading edge, and $x=D(z)/2$ to the trailing edge. The z axis (perpendicular to $\vec{\mathbf{\Omega}}_T$) has origin at the rotation axis and runs along the middle of the wing span. In this rotating system the flow has a background constant vorticity $-2\vec{\mathbf{\Omega}}_T$ plus regions of highly concentrated vorticity, modeled as appropriate singularities of a potential flow, so that we write the velocity as the sum of a uniformly rotating flow plus a potential part [9]

$$\mathbf{u} = -\vec{\mathbf{\Omega}}_T \times \mathbf{x} + \nabla \phi. \tag{1}$$

The incompressibility condition $\nabla \cdot \mathbf{u} = 0$ implies that ϕ satisfies the Laplace equation $\nabla^2 \phi = 0$. Besides, as far away from the plate the flow is $\mathbf{u} = -\vec{\mathbf{\Omega}}_T \times \mathbf{x}$, ϕ has to grow more slowly than linearly with the distance from the wing as $|\mathbf{x}| \to \infty$. On the other hand, the boundary condition at the wing is zero normal velocity ($u_y = 0$) so that, from Eq. (1), we can write ($\mathbf{\Omega}_T \equiv |\vec{\mathbf{\Omega}}_T|$)

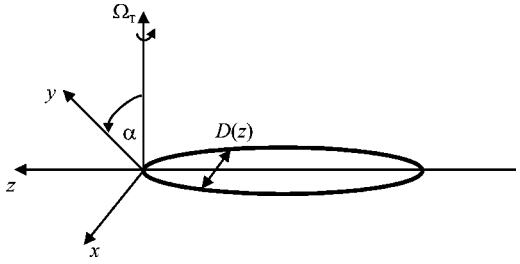

FIG. 1. Sketch showing the rotating wing, coordinate system, and conventions used.

$$\left.\frac{\partial \phi}{\partial y}\right)_{\text{wing}} = \vec{\mathbf{\Omega}}_T \times \mathbf{x})_{\text{wing}} = \Omega_T z \sin\alpha.$$

These boundary conditions suggest to seek a potential of the form

$$\phi = -\Omega_T z[\phi_0(x,y) - x\cos\alpha - y\sin\alpha], \tag{2}$$

where $\phi_0(x,y)$ is the two-dimensional potential corresponding to the fluid with velocity components $U_{0x}=\cos\alpha$, $U_{0y}=\sin\alpha$, away from the wing. This is the usual approximation of blade element theory [10] that models the two-dimensional flow in each section $z=$const of the plate, as if it moved with a translational velocity $U_x=\mathbf{\Omega}_T z\cos\alpha$, $U_y=\mathbf{\Omega}_T z\sin\alpha$. This approach neglects curvature effects in each $z=$const section of the wing, which is a very good approximation except very close to the rotation axis. It is then immediate to see that the potential (2) satisfies the Laplace equation and the correct boundary conditions.

The two-dimensional flow potential $\phi_0(x,y)$ can be readily obtained using complex variable techniques. The complex potential for the flow considered is given in terms of the transformed variable ζ as [7]

$$\omega_0(\zeta) = U_0^*\zeta + U_0\frac{a^2}{\zeta} + \frac{\Gamma^0+\Gamma_v^0}{2\pi i}\ln\zeta + \frac{\Gamma_v^0}{2\pi i}\ln(\zeta-\zeta_v) - \frac{\Gamma_v^0}{2\pi i}\ln\left(\zeta - \frac{a^2}{\zeta_v^*}\right), \tag{3}$$

where $U_0=\cos\alpha+i\sin\alpha$, $a=D(z)/4$, Γ^0 is the circulation around the plate, and Γ_v^0 and ζ_v the circulation and position, respectively, of the LEV. The relation between the complex variables $Z\equiv x+iy$ and ζ is given by the Joukowski function

$$Z = \zeta + \frac{a^2}{\zeta}. \tag{4}$$

As shown in [7] the circulations Γ^0 and Γ_v^0 are determined by Kutta-Joukowski conditions $d\omega_0/dz=0$ at both edges $\zeta=\pm a$. The upper indices 0 indicate that these circulations are those corresponding to U_0, a dimensionless magnitude, so that both circulations have units of length. Actual circulations have values $-\mathbf{\Omega}_T z\Gamma_v^0$ and $-\mathbf{\Omega}_T z\Gamma^0$.

Note that $\phi_0(x,y)$ picks up an implicit dependence on z through a and ζ_v if these parameters depend on z. So, as long as the chord length and the vortex position vary slowly with z, the strongest z dependence is that explicitly considered, and Eq. (2) is a good representation of the flow.

The potential $\phi_0(x,y)$ can now be determined as

$$\phi_0(x,y) = \mathrm{Re}[\omega_0(\zeta(Z))]. \tag{5}$$

The resulting z-component of the velocity relative to the wing is then

$$u_z = -(\vec{\mathbf{\Omega}}_T \times \mathbf{x})\cdot\mathbf{e}_z + \frac{\partial\phi}{\partial z} = 2\Omega_T(x\cos\alpha + y\sin\alpha) - \Omega_T\,\mathrm{Re}[\omega_0(\zeta(Z))].$$

Besides, as $\mathrm{Re}[U_0^*Z]=x\cos\alpha+y\sin\alpha$, we can define an auxiliary potential

$$\omega_{aux}(\zeta) \equiv \omega_0(\zeta) - 2U_0^*\left(\zeta + \frac{a^2}{\zeta}\right), \tag{6}$$

so that u_z can be written as

$$u_z = -\Omega_T\,\mathrm{Re}[\omega_{aux}(\zeta(Z))]. \tag{7}$$

This expression is not yet final because the potential ϕ_0 is not completely defined as an arbitrary constant can be added to it. One can determine this additive constant using the condition that the net flow across any $z=$const plane has to be finite, as the finite wing cannot force the flow of an infinite mass of fluid. At large values of x and/or y the expression of u_z is given by

$$u_z \to \Omega_T(x\cos\alpha + y\sin\alpha) - \Omega_T\frac{\Gamma^0+\Gamma_v^0}{2\pi}\varphi,$$

where φ is the argument of ζ, measured from the x axis. The integral of the terms $x\cos\alpha$ and $y\sin\alpha$ cancel by symmetry, so that for the integral of u_z across the $z=$const plane to be finite, it is readily seen that a constant of value $\mathbf{\Omega}_T(\Gamma^0+\Gamma_v^0)/2$ must be added to the expression of u_z given by Eq. (7).

Finally, note that because of the z-dependence of translational velocity of each section of the wing, a z-dependent circulation results. This, in turn, makes the velocity u_z discontinuous, with discontinuity

$$\Delta u_z = -\Omega_T(\Gamma^0+\Gamma_v^0), \tag{8}$$

across a vorticity sheet shed at the trailing edge [11]. To fix the discontinuity surface at the trailing edge we must adopt the convention that the branch of the function $\ln\zeta$ in Eq. (3) corresponds to the line $\mathrm{Im}[\zeta]=0$, $\mathrm{Re}[\zeta]>0$. With all this we finally have

$$u_z = -\Omega_T\,\mathrm{Re}[\omega_{aux}(\zeta(Z))] + \Omega_T\frac{\Gamma^0+\Gamma_v^0}{2}, \tag{9}$$

together with expressions (3) and (6).

The resulting flow structure corresponds to a highly compact vortex that models the observed region of concentrated vorticity. This vorticity originates in the leading edge and is fed to the vortex through a vortex sheet connecting the vortex and the edge. The vorticity content of this sheet is expected to be low in the stationary regime, when a stable LEV is well developed, because the flow regularization near the leading edge, due to the LEV itself, should lead to a low rate of vorticity emission from this edge. We will see later that only when this rate is sufficiently small can it be balanced by the effect of the flow u_z, which can happen only at particular positions of the vortex

Since the circulation varies along the vortex, an essentially three-dimensional structure must exist, with vorticity vector components along z and also in the plane perpendicular to z. We should then more precisely speak of the circulation associated to the z-component of vorticity. The variation of vortex circulation implies also the variation of the circulation along the wing, which requires, by a direct application of Stokes theorem [12], that the velocity along the wing has a discontinuity, the jump given by Eq. (8). This velocity

jump, indirect evidence of a z-dependent circulation, is well documented in Fig. 1(c) of Ref. [2], where isolines of spanwise velocity are shown. A marked variation of velocity across a thin region in the rear of the wing is clearly shown in that figure.

III. VORTICITY EVOLUTION

Consider now the evolution of vorticity $\vec{\omega}=\boldsymbol{\nabla}\times\mathbf{u}$ in the rotating system, at high Reynolds number, governed by the equation [12]

$$\frac{\partial\vec{\omega}}{\partial t}+(\mathbf{u}\cdot\boldsymbol{\nabla})\vec{\omega}=(\vec{\omega}\cdot\boldsymbol{\nabla})\mathbf{u}+2(\vec{\boldsymbol{\Omega}}_T\cdot\boldsymbol{\nabla})\mathbf{u}.$$

If we write $\vec{\omega}=-2\vec{\boldsymbol{\Omega}}_T+\vec{\omega}'$ to make explicit the concentrated (or absolute) vorticity $\vec{\omega}'$, and consider the z-component of the above equation, we obtain

$$\frac{\partial\omega_z'}{\partial t}+\boldsymbol{\nabla}_\perp\cdot(\mathbf{u}_\perp\omega_z')=\boldsymbol{\nabla}_\perp\cdot(\vec{\omega}_\perp' u_z), \tag{10}$$

where the symbol $\perp$ refers to the plane (x,y) transverse to $\mathbf{e}_z$.

Since

$$\boldsymbol{\nabla}_\perp\cdot(\vec{\omega}_\perp' u_z)=u_z\boldsymbol{\nabla}_\perp\cdot\vec{\omega}_\perp'+\vec{\omega}_\perp'\cdot\boldsymbol{\nabla}_\perp u_z=-u_z\frac{\partial\omega_z'}{\partial z}+\vec{\omega}_\perp'\cdot\boldsymbol{\nabla}_\perp u_z, \tag{11}$$

the right-hand side of Eq. (10) includes the effects of advection of ω_z' by the spanwise flow u_z, represented by the first term in the right-hand side of Eq. (11), and of tilting and stretching of transverse vorticity $\vec{\omega}_\perp'$ by the same flow, the second term in the right-hand side of Eq. (11). Analogously, for the second term in the left-hand side of Eq. (10), since the transverse flow $\mathbf{u}_\perp$ is itself solenoidal, from Eq. (2), we have

$$\boldsymbol{\nabla}_\perp\cdot(\mathbf{u}_\perp\omega_z')=\mathbf{u}_\perp\cdot\boldsymbol{\nabla}_\perp\omega_z'$$

that represents the advection of ω_z' by the transverse flow.

If Eq. (10) is integrated on a transverse surface S that includes all concentrated vorticity associated to the LEV, for instance, the region inside the instantaneous streamline shown in Fig 2, the transverse divergence term in the left-hand side leads by Gauss theorem to (C is the curve limiting the surface)

$$\int_S\boldsymbol{\nabla}_\perp\cdot(\mathbf{u}_\perp\omega_z')dS=\oint_C\omega_z'\mathbf{u}_\perp\cdot\mathbf{n}dl.$$

Only the inflow of z-vorticity generated at the solid boundary contributes to this last integral

$$\int_S\boldsymbol{\nabla}_\perp\cdot(\mathbf{u}_\perp\omega_z')dS=-\left.\frac{d\Gamma_z}{dt}\right|_B, \tag{12}$$

where Γ_z is the integral of ω_z' over S, and $d\Gamma_z/dt|_B$ represents its instantaneous rate of change by generation at the boundary B.

Analogously, we have for the transverse divergence term in the right-hand side

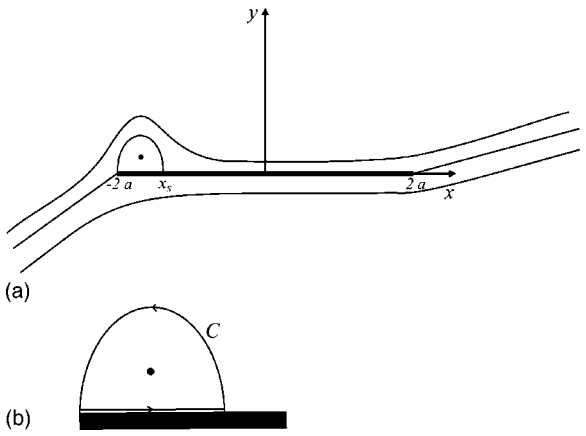

FIG. 2. (a) Two-dimensional streamlines, and (b) detail with contour used to obtain Eq. (14).

$$\int_S\boldsymbol{\nabla}_\perp\cdot(\vec{\omega}_\perp' u_z)dS=\oint_C u_z\vec{\omega}_\perp'\cdot\mathbf{n}dl, \tag{13}$$

to which, as before, only contributes the section of C that coincides with the solid boundary. Since the vorticity in the boundary layer due to the flow over the wing is perpendicular to $\mathbf{n}$, the only component of concentrated vorticity that has a component along $\mathbf{n}$ is that due to rotation, as the fluid in contact with the solid is forced to rotate with angular velocity $\vec{\boldsymbol{\Omega}}_T$, with corresponding vorticity $2\vec{\boldsymbol{\Omega}}_T$. We thus have

$$\oint_C u_z\vec{\omega}_\perp'\cdot\mathbf{n}dl=-2\vec{\boldsymbol{\Omega}}_T\cdot\mathbf{e}_y\int_{-2a}^{x_S}u_z dx=-2\Omega_T\cos\alpha\int_{-2a}^{x_S}u_z dx,$$

where x_S is the x-coordinate of the stagnation point of the flow over the wing (see Fig. 2).

We obtain in this way,

$$\frac{\partial\Gamma_z}{\partial t}=\left.\frac{d\Gamma_z}{dt}\right|_B-2\vec{\boldsymbol{\Omega}}_T\cdot\mathbf{e}_y\int_{-2a}^{x_S}u_z dx. \tag{14}$$

The Γ_z in this equation represents the circulation of the z-component of concentrated vorticity, which is modeled as the corresponding singularity of the potential (2), expressed as

$$\Gamma_z=-\Omega_T z\Gamma_v^0.$$

To obtain an expression for $d\Gamma_z/dt|_B$ we take into account that the vorticity shed at the leading edge is that necessary to ensure the Kutta-Joukowski condition at that boundary when the configuration of the flow changes. This happens in the solution (3) as the vortex in ζ_v moves advected by the transverse flow. We note here that the vortex is always advected by the transverse flow as there are no stagnation points in the regions considered. To look for regions with a stationary vorticity distribution, where the continuous generation of vorticity at the leading edge is balanced by the effect of the spanwise flow, we approximate the value of $d\Gamma_v^0/dt$ as that associated to the free motion of the vortex even at those locations. This is better justified later as it is found that only extremely close to the locations of stationary vorticity does

the last term in Eq. (14) become comparable to $d\Gamma_z/dt|_B$, so that the transverse motion of the vortex proceeds unaffected, advected by the transverse flow, until very close to the mentioned regions. In this way we have

$$\frac{d\Gamma_v^0}{dt} = \frac{\partial \Gamma_v^0}{\partial \zeta_v}\frac{d\zeta_v}{dt} + \frac{\partial \Gamma_v^0}{\partial \zeta_v^*}\frac{d\zeta_v^*}{dt},$$

where we have used for convenience ζ_v and its complex conjugate ζ_v^* as independent variables, instead of $\mathrm{Re}(\zeta_v)$ and $\mathrm{Im}(\zeta_v)$, and where

$$\frac{d\zeta_v^*}{dt} = \left(\frac{d\zeta_v}{dt}\right)^* = -\Omega_T z \frac{d\hat{\omega}_0}{d\zeta}\bigg)_{\zeta_v} \left|\frac{dZ}{d\zeta}\bigg)_{\zeta_v}\right|^{-2},$$

with

$$\hat{\omega}_0(\zeta) \equiv \omega_0(\zeta) - \frac{\Gamma_v^0}{2\pi i}\ln[Z(\zeta) - Z(\zeta_v)]. \tag{15}$$

The last two expressions result when one relates the motion of ζ_v to the motion of the true vortex (that in the Z-plane), but expressed in terms of the potential obtained in the ζ-plane, which is sometimes referred to as the Routh theorem [13,14]. We can then write

$$\left.\frac{d\Gamma_z}{dt}\right|_B = 2(\Omega_T z)^2 \left|\frac{dZ}{d\zeta}\bigg)_{\zeta_v}\right|^{-2} \mathrm{Re}\left[\frac{\partial \Gamma_v^0}{\partial \zeta_v^*}\frac{d\hat{\omega}_0}{d\zeta}\bigg)_{\zeta_v}\right]. \tag{16}$$

In summary, we arrive at the following picture of the dynamics of the vortex. There is a growth due to the vorticity generated at the leading edge that is transported to the vortex by the transverse flow. This transverse flow only advects the z-component of vorticity without changing its associated circulation Γ_z, and so all corresponding circulation generated at the leading edge (by release of ω_z from the boundary layer) is fed to the vortex, what is expressed by Eq. (12). The spanwise flow u_z, in turn, has a more complex effect. It advects along the wing the z-component of vorticity, the first term in the right-hand side of Eq. (11), and also stretches and tilts the perpendicular components of vorticity (the second term in the same equation) so as to increase or decrease the circulation Γ_z associated to ω_z.

IV. VORTICITY DISTRIBUTION AND STABILITY

We look now for the stationary solutions of Eq. (14). Note first that, as Γ^0 and Γ_v^0 are proportional to a, if one defines dimensionless variables

$$\gamma \equiv \Gamma^0 a^{-1}, \quad \gamma_v \equiv \Gamma_v^0 a^{-1},$$

$$\xi \equiv \zeta a^{-1}, \quad \xi_v \equiv \zeta_v a^{-1},$$

$$\varpi \equiv \hat{\omega}_0 a^{-1}, \quad \tilde{u}_z \equiv u_z(\Omega_T a)^{-1},$$

$$\tilde{x} \equiv x a^{-1}, \quad \tilde{x}_S \equiv x_S a^{-1}$$

and uses Eqs. (3), (4), and (15) and the expressions of the circulations Γ^0 and Γ_v^0 [7], the condition for stationary equilibrium can be written in nondimensional form as

$$-2\cos\alpha\int_{-2}^{\tilde{x}_S}\tilde{u}_z d\tilde{x} = 2\left(\frac{z}{a}\right)^2 \frac{|\xi_v|^4}{|\xi_v^2 - 1|^2} \times \mathrm{Re}\left[\frac{\partial \gamma_v}{\partial \xi_v^*}\frac{d\varpi}{d\xi}\bigg)_{\xi_v}\right], \tag{17}$$

where

$$\varpi(\xi) = e^{-i\alpha}\xi + \frac{e^{i\alpha}}{\xi} + \frac{\gamma + 2\gamma_v}{2\pi i}\ln\xi - \frac{\gamma_v}{2\pi i}\ln\left(\xi - \frac{1}{\xi_v}\right) - \frac{\gamma_v}{2\pi i}\ln\left(\xi - \frac{1}{\xi_v^*}\right),$$

$$\gamma_v = 8\pi\sin\alpha\left[\frac{1 - \xi_v\xi_v^*}{(1+\xi_v)(1+\xi_v^*)} - \frac{1 - \xi_v\xi_v^*}{(1-\xi_v)(1-\xi_v^*)}\right]^{-1},$$

$$\gamma = -\frac{\gamma_v}{2}\left[2 + \frac{1 - \xi_v\xi_v^*}{(1+\xi_v)(1+\xi_v^*)} + \frac{1 - \xi_v\xi_v^*}{(1-\xi_v)(1-\xi_v^*)}\right].$$

In this way, all Ω_T dependence disappears, so that given only the values of α and z/a, relation (17) determines a curve in the ξ-plane over which a stationary distribution of vorticity can exist. A first point to be noted is that the right-hand side of relation (17) turns out to be in magnitude much larger than the left-hand side, except in a narrow region where it rapidly decreases. This behavior indicates that the joint action of advection and vortex stretching and tilting by the spanwise flow is important only in very localized regions, giving *a posteriori* justification for the whole approach and, in particular, to the derivation of Eq. (16). Another important consequence is that the region of equilibrium is practically independent of z (for instance, for $\alpha = 45°$ changes of z/a between 2 and 20 lead to changes below 1% in ξ_v, with similar variations for other angles of attack). This weak z-dependence is related to the z-independence of all factors, other than $(z/a)^2$, in the right-hand side of Eq. (17), which results in turn from the assumptions leading to the flow velocity (9). In this sense we obtain a self-consistent approach, but it does not exclude the possibility of more complex flow structures, with pronounced z-dependence. These structures are likely to exist, probably depending on the Reynolds number.

The second point is that only over a localized portion of the curve, near the position of the leading edge, $\xi_l = -1$, is the equilibrium stable. To study this, we consider small perturbations $\delta\xi$ of the location of the vortex around an equilibrium position ξ_{v0}, and write the nondimensional version of Eq. (14) linearized about ξ_{v0} as

$$-\frac{z}{a}\frac{\partial \delta\gamma_v}{\partial \tau} = \frac{\partial A}{\partial \xi_v}\bigg)_{\xi_{v0}}\delta\xi + \frac{\partial A}{\partial \xi_v^*}\bigg)_{\xi_{v0}}\delta\xi^*,$$

where $\delta\gamma_v$ is the variation of γ_v with respect to its equilibrium value, $\tau = \Omega_T t$, and A represents the nondimensional version of the right-hand side of Eq. (14) [A is equal to the right-hand side of Eq. (17) minus its left-hand side]. We define an equilibrium situation as stable if, for $\delta\gamma_v > 0$ one

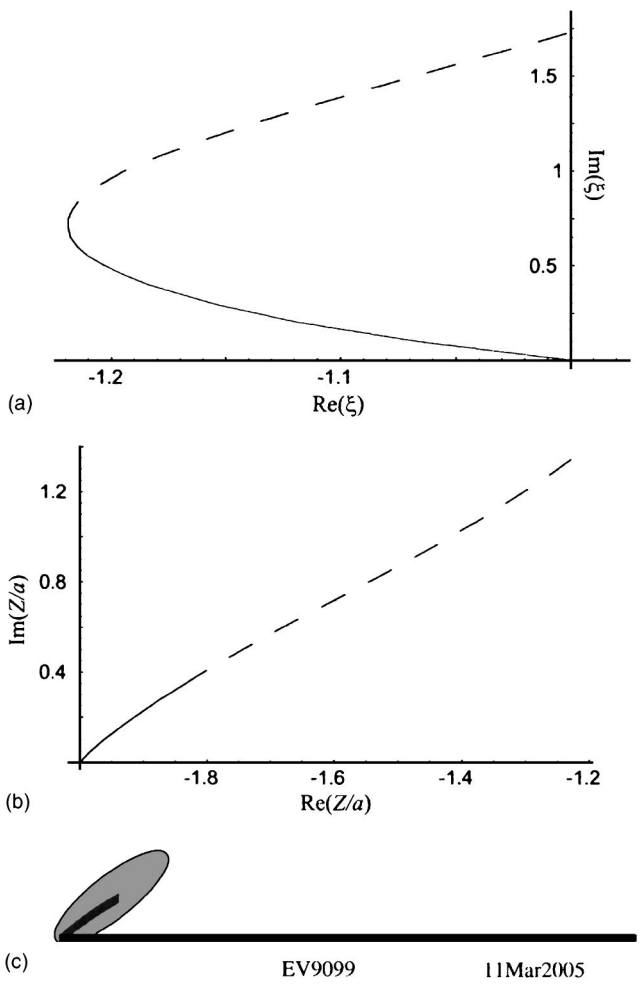

FIG. 3. (a) Equilibrium curve in the ξ-plane and (b) corresponding curve in the Z/a-plane. Full lines denote stable equilibrium sections and dashed lines unstable ones. (c) Region of stable equilibrium relative to the wing section, for $\alpha=45°$ and $z/a=4$, represented with a full line, together with the region of intense vorticity shown in deep blue color in Fig. 1(b) of Ref. [2], represented as a gray zone.

has $\partial\delta\gamma_v/\partial\tau<0$, and for $\delta\gamma_v<0$ one has $\partial\delta\gamma_v/\partial\tau>0$; that is, $\delta\gamma_v\partial\delta\gamma_v/\partial\tau<0$. Since

$$\delta\gamma_v = \left.\frac{\partial\gamma_v}{\partial\xi_v}\right)_{\xi_{v0}}\delta\xi + \left.\frac{\partial\gamma_v}{\partial\xi_v^*}\right)_{\xi_{v0}}\delta\xi^*,$$

remembering that $z<0$, we write the stable equilibrium condition as

$$\mathrm{Re}\left[\left.\frac{\partial A}{\partial\xi_v}\right)_{\xi_{v0}}\delta\xi\right]\mathrm{Re}\left[\left.\frac{\partial\gamma_v}{\partial\xi_v}\right)_{\xi_{v0}}\delta\xi\right]<0$$

for any $\delta\xi$. Written in terms of Re ξ and Im ξ this condition is easily checked through the negative definite character of the resulting matrix of real coefficients.

In Fig. 3 we show the equilibrium curve in the ξ-plane for $\alpha=45°$ and $z/a=4z/D=4$ [Fig. 3(a)], together with the corresponding curve in the Z/a plane [Fig. 3(b)]. The stable region is indicated by a full line, while the dashed line corresponds to the unstable part. The magnitude of vortex circulation increases monotonically along the curve. We can then expect in an actual wing a distribution of vorticity along the stable section of the curve indicated, with increasing intensity towards the curve's end. In fact, the experimental vorticity distribution shown in Fig. 1(b) of Ref. [2], that corresponds to the same angle of attack, has a striking similarity (in position, shape, and extension) to Fig. 3(c), where the stable equilibrium region is shown relative to the wing section, together with the zone of intense vorticity observed in the experiment. The end of the stable region, where the most intense stable vortex can exist, coincides very well with the center of the core of intense vorticity observed in[2] (this center is marked with a star in that reference). The gray zone in Fig. 3(c) corresponds to that shown in deep blue color in the cited reference.

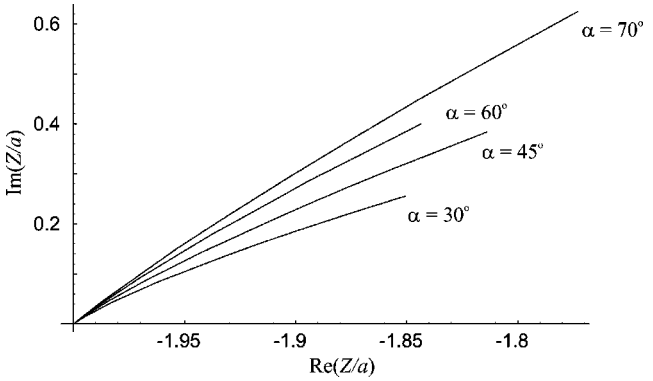

FIG. 4. Stable equilibrium curves in the Z/a-plane for different angles of attack.

To make a quantitative comparison, consider an average position of the vortex weighted by vortex magnitude,

$$\xi_{\mathrm{average}} \equiv \frac{\int \gamma_v(s)\xi_v(s)ds}{\int_v \gamma_v(s)ds},$$

where s is the length along the equilibrium curve, and the integral is extended only to the stable section. For $\alpha=45°$ we obtain $\xi_{\mathrm{average}}\simeq -1.20+i0.52$, which can be compared with the value $-1.25+i0.48$ used in Ref. [7] to reproduce experimental results.

Finally, Fig. 4 shows the stable equilibrium curves in the Z/a plane, for different angles of attack, all for $z/a=4$. The differences are not large for angles around 45°, but for $\alpha\simeq 70°$ the stable region increases and for $\alpha\gtrsim 75°$ (not shown) it extends indefinitely. This behavior would indicate an extended region of stationary vorticity at angles of attack above 75°, which would be interesting to verify experimentally.

V. CONCLUSIONS

An analytical study of the stationary distribution of leading-edge vorticity was presented. It is shown that the

basic fact of wing rotation around its root generates a spanwise flow intense enough to maintain a stationary (relative to the wing) vortex, due to the balance between vorticity advection, tilting, and stretching by this flow, and vorticity generation at the leading edge, as put forward some time ago [3]. The considerations of constant angular velocity and fixed angle of attack apply during most of each half-stroke in a typical insect flapping sequence [15]. The approximation of constant wing chord, use of blade element theory, and neglect of wing-end effects are necessary for the analytical approach, and can be justified in usual insect wings in their midsections, where substantial lift is generated [6]. The wing-end effects require a further discussion. We originally conjectured that the main spanwise flow was produced by the tip vortex that necessarily exists in any finite, lift-generating wing [11]. However, no reasonable model of this vortex was able to induce a sufficiently strong flow to stabilize the vortex growth in most of the wing, only very close to the tip. As a result we were led to consider the induction of the spanwise flow by rotation of the wing. The conclusion was then that the tip vortex does affect the flow in its vicinity, but cannot induce the stabilizing flow in most of the wing. Probably related to this point is the observation [16] that the LEV detaches at approximately 75% of the wing length, where the influence of the tip vortex cannot be ignored. In this sense Fig. (1d) of Ref. [2] is very suggestive as it shows the tip vortex occupying approximately the last 25% of the wing length. Wing-end effects should certainly be included in a more realistic model of LEV dynamics, although the analytical approach is difficult because of the strong three-dimensional features of the flow near the wing tip.

With all the above assumptions we identify a region close to the leading edge where a stable stationary vorticity distribution can exist that compares very well qualitatively and quantitatively with experiments and previous theoretical approaches. Besides, extended regions of vorticity are predicted for large angles of attack (above 75°), a point worth verifying experimentally.

ACKNOWLEDGMENT

The authors acknowledge grants of the CONICET and the University of Buenos Aires.

[1] M. H. Dickinson, F.-O. Lehmann, and S. P. Sane, Science **284**, 1954 (1999).
[2] J. M. Birch and M. H. Dickinson, Nature (London) **412**, 729 (2001).
[3] T. Maxworthy, J. Fluid Mech. **93**, 47 (1979).
[4] T. Maxworthy, Annu. Rev. Fluid Mech. **13**, 329 (1981).
[5] H. Liu, C. P. Ellington, C. V. D. Berg, and A. P. Willmott, J. Exp. Biol. **201**, 461 (1998).
[6] R. Ramamurti and W. C. Sandberg, J. Exp. Biol. **205**, 1507 (2002).
[7] F. O. Minotti, Phys. Rev. E **66**, 051907 (2002).
[8] S. P. Sane and M. H. Dickinson, J. Exp. Biol. **205**, 1087 (2002).
[9] F. O. Minotti, Phys. Fluids **15**, 3576 (2003).
[10] F. E. Weick, NACA Technical Note No. 235 (1926).
[11] A. M. Kuethe and C. Yen Chow, *Foundations of Aerodynamics* (Wiley, New York, 1986).
[12] G. K. Batchelor, *An Introduction to Fluid Dynamics* (Cambridge University Press, Cambridge, England, 2000).
[13] L. M. Milne-Thomson, *Theoretical Hydrodynamics* (Macmillan, New York, 1968).
[14] M. Karweit, Phys. Fluids **18**, 1604 (1975).
[15] J. M. Wakeling and C. P. Ellington, J. Exp. Biol. **200**, 557 (1997).
[16] C. van den Berg and C. P. Ellington, Philos. Trans. R. Soc. London, Ser. B **352**, 329 (1997).